Topological Overview of Powertrains for Battery-Powered Vehicles With Range Extenders

Ilan Aharon and Alon Kuperman, *Member, IEEE*

***Abstract*—The paper presents a topological overview of hybrid powertrains for battery-powered vehicles reinforced by range extenders. First, tradeoffs of employing high energy versus high power battery are revealed. Then, different topologies of battery–ultracapacitor hybrids are discussed, highlighting pros and cons of each configuration. The superiority of fully active hybrids is indicated, obtained at the expense of increase of power electronic circuitry, control effort, and efficiency. The second part of the paper focuses on two types of range extenders: renewable energy and fuel-based units. The operation strategy is shown to be different for each range extender type. The renewable-energy-based range extender should be operated employing either passive or active maximum power point tracking strategy and hence not be involved in the powertrain energy balancing. It is shown that such a strategy allows the rest of system to perceive the renewable energy range extender (RERE) as a part of the load and act accordingly. Solar array is given as an example of a RERE and the possible connection topologies are discussed. On the other hand, the fuel-based range extender (FBRE) should be operated near the lowest specific fuel consumption point employing maximum efficiency point tracking strategy. Fuel cells and internal combustion engines are specified as examples of FBREs. The complete powertrain is shown to resemble a dc microgrid with source, storage, and load units connected through power management circuitry to a common dc link.**

***Index Terms*—Batteries, dc microgrids, electric propulsion, electric vehicles, fuel cells, internal combustion engines (ICEs), power converters, range extenders, renewable energy, ultracapacitors.**

I. Introduction

SINCE the comprehensive recognition of the global warming as well as emissions devastating effects and awareness of the fact that despite fossil fuels resources limitations, the demand for oil increases [1], enormous efforts are invested in development of electric, more electric, hybrid, and plug-in hybrid vehicles. The road transportation has been so far the most popular field of research [2]–[11], while aerial [12]–[15] and marine [16]–[18] vehicles also attracted much of the researchers' attention. For the road transportation, topological overview of hybrid electric and fuel cell vehicular power system architectures and configurations was presented in [2] and [11], while power electronics and motor drives involved were demystified in [4] and [8]. Comprehensive efficiency analysis was performed in [3], [5], and [6], and modeling/design methodologies were proposed in [7], [9], and [10]. More electric and hybrid aircraft topologies were proposed as an alternative to conventional aerial vehicles in [12], while the discussion on the possible alternative power sources and the expected tradeoffs was presented in [13] and [14]. The feasibility of hybrid propulsion system for a small aircraft was demonstrated in [15]. Comparison of submarine hybrid drive topologies was performed in [16]; modeling and design methodologies of electric and fuel cell marine vehicles were recommended in [17] and [18], respectively. As a conclusion of the research done by now, electric vehicles are probably the most desired form of transportation for both civilian and military vehicles. From the civilian point of view, zero emissions at the populated area and the absence of hazardous flammable fuels onboard are perhaps the most eye-catching characteristics. From the military side, low noise and thermal signature of electric vehicles are the attractive features. However, the energy storage technology in general and battery technology in particular is the bottleneck preventing the widespread of all-electric vehicles. The main disadvantage of such vehicles is a comparatively low operation range/mission duration requiring highly dense fuel stations infrastructure in case of road vehicles and preventing high endurance missions in case of aerial/marine vehicles. The present solution is hybridizing the conventional vehicles by reducing the fuel-based engine rating, while increasing the electrical energy storage and propulsion units [19], [20]. An alternative answer is hybridizing the electric vehicles by optimizing the energy storage unit and reinforcing the powertrain with range extenders. In such a vehicle, the energy storage unit is able to provide the power required by the vehicle loads, however its energy content is insufficient to offer a desired operation range. Hence, the range extenders employed are used to supply the excess energy in order to provide the additional amount of endurance to the loads. The rating of the range extenders is lower than the energy storage rating, as opposite to the hybrid vehicle case. This paper discusses the approaches to optimize the energy storage unit by hybridization and describes two kinds of range extenders: renewable energy and fuel-based units. Solar arrays, for example, while insufficient for road vehicles, may easily supply around 10% of the cruising energy required by an unmanned aerial vehicle with appropriate wingspan. Fuel cells are high energy density sources and are characterized by near zero emissions. Both sources are considered as possible range extenders.

From the system point of view, a hybrid powertrain can be perceived as a dc microgrid, containing source, storage, and

Manuscript received July 1, 2010; revised October 13, 2010; accepted January 4, 2011. Date of current version May 13, 2011. Recommended for publication by Associate Editor M. Liserre.

The authors are with the Department of Electrical Engineering and Electronics, Hybrid Energy Sources Laboratory, Ariel University Center, Ariel, 40700 Israel (e-mail: ilanah@ariel.ac.il, alonku@ariel.ac.il).

Color versions of one or more of the figures in this paper are available online at http://ieeexplore.ieee.org.

Digital Object Identifier 10.1109/TPEL.2011.2107037

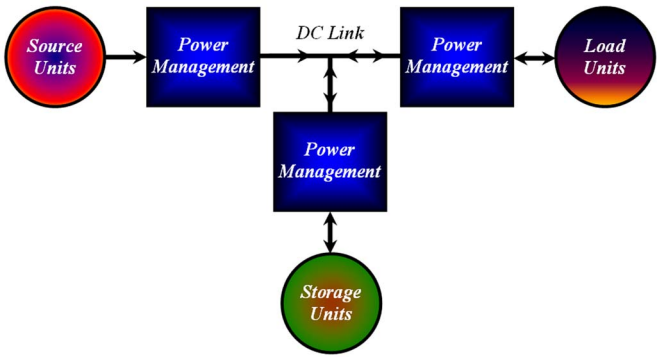

Fig. 1. DC microgrid: A system point of view.

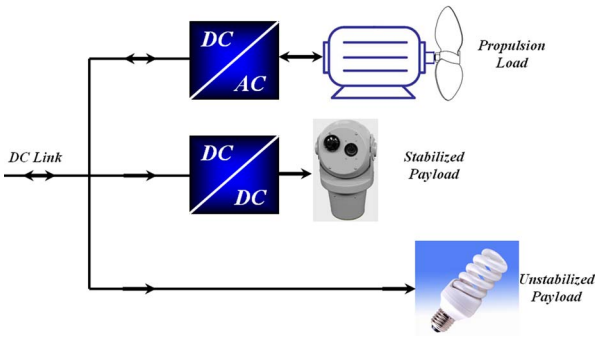

Fig. 2. Typical vehicle load.

load units, each connected via power management circuitry to a common dc link, through which the power flow occurs, as shown in Fig. 1. Note that the power management circuitry may include either power electronic converter or simple switches/fuses to allow direct connection of a source/storage/load unit to the dc link.

The direction of power flow of each unit is indicated in Fig. 1. While the source units are capable of supplying energy only, the storage and the load units of electric vehicles are bidirectional. Since the load unit possesses regenerative braking capability, the storage unit must maintain the power balance of the dc link. The similarity between the vehicle powertrains and microgrids allows utilizing power electronics topologies [21] as well as power management strategies used in microgrids [22], [23] for managing the vehicle power flow.

The rest of the manuscript is arranged as follows. Section II presents typical vehicle load characteristics, requirements, and limitations. Section III describes battery-powered vehicles, while electric vehicles with hybridized energy storage units are discussed in Section IV. Different topologies are shown and the advantages/disadvantages of each are clearly highlighted. The range extension approach is presented in Section V and the topologies of the two kinds of range extenders are explained. The paper is concluded in Section VI.

II. Typical Vehicle Load

An electric vehicle load typically consists of three main subunits: propulsion motor, stabilized, and unstabilized payloads, as shown in Fig. 2. The propulsion motor (typically, a permanent magnet synchronous machine) is connected to the dc link via a controlled dc/ac converter (inverter) and is the main load of the vehicle, seen as a constant power load by the rest of the powertrain [24]. The stabilized payload is also connected to the dc link via a power electronic converter, usually of a dc–dc type. Typical examples of stabilized payloads are electronic weapon systems or surveillance cameras. The unstabilized loads, such as lights are connected directly to the dc link via some kind of protection circuitry (not shown in Fig. 2) and typically act as constant resistance loads.

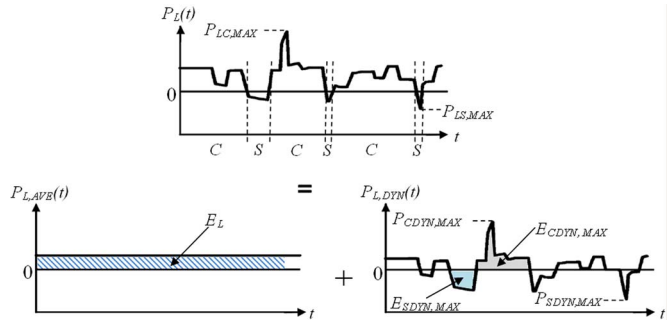

Fig. 3. Vehicle load power profile decomposition.

Therefore, a typical vehicle load can be generally characterized as a constant power load. In addition, the electric vehicles load is characterized by bidirectional power flow, since it supports regenerative braking capability. In order to fully understand the requirements of such a load, consider a consumption profile given in Fig. 3, defining the energy and power load requirements. The consumption or power profile is the load power versus time $P_L(t)$ seen from the dc link. Note that most of the time the load is consuming power (C), while there are some bursts of power supplied (S) by the load to the system. The amount of the regenerated energy depends on the type of the vehicle. The regenerative energy is relatively high in the road vehicles during the urban driving cycle. On the contrary, aerial vehicles are capable of regenerating only during infrequent braking of altitude reduction. According to Fig. 3, denote $P_{LC,\mathrm{MAX}}$ as the maximum consumed load power during traction and $P_{LS,\mathrm{MAX}}$ as maximum supplied load power during regeneration. In order to operate the load correctly, the sources and energy storage units must be able to satisfy these load power demands.

The instantaneous load power can be decomposed into two components, as shown in Fig. 3 [25]: steady (average) power and dynamic power with zero average

$$P_L(t) = P_{L,\mathrm{AVE}}(t) + P_{L,\mathrm{DYN}}(t). \tag{1}$$

When a single source is employed, it must supply both components. In a hybrid vehicle, the powertrain contains several sources/energy storages, some favoring steady-state operation, and hence, supplying the average power $P_{L,\mathrm{AVE}}$; other are used to supply the dynamic power $P_{L,\mathrm{DYN}}$. Note that the overall energy of the dynamic powertrain will be theoretically zero in a whole driving cycle. This implies that the energy source of the dynamic powertrain does not lose energy capacity at the end

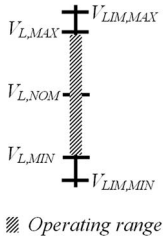

Fig. 4. Vehicle load voltage operating range.

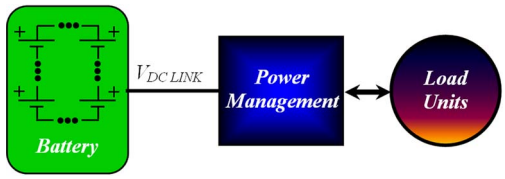

Fig. 5. Battery-powered electric vehicle powertrain.

of the driving cycle (if the internal losses are neglected), functioning as a power damper only [25]. In practice, any source has some amount of internal losses, which are compensated by drawing some energy from the steady-state power source. The energy demand of the load is given by

$$E_L = \int_0^{T_M} P_{L,\mathrm{AVE}}(x)dx = P_{L,\mathrm{AVE}} \times T_M \tag{2}$$

where T_M is the mission/driving duration. The actual energy demand is a bit higher if the dynamic powertrain losses are taken into account. According to Fig. 3, denote $P_{\mathrm{CDYN,MAX}}$ as the maximum consumed dynamic load power and $P_{\mathrm{SDYN,MAX}}$ as the maximum supplied dynamic load power. Hence, the dynamic powertrain must be able to supply $P_{\mathrm{CDYN,MAX}}$ and absorb $P_{\mathrm{SDYN,MAX}}$. In addition, the dynamic powertrain must have some capability of energy storage. From Fig. 3, the dynamic powertrain must be able to supply $E_{\mathrm{CDYN,MAX}}$ and store $E_{\mathrm{SDYN,MAX}}$. Another load requirement is the dc-link voltage range. Power electronics feeding the load units must typically operate within a predetermined voltage range ($V_{\mathrm{LIM,MIN}}$ to $V_{\mathrm{LIM,MAX}}$) with a nominal voltage $V_{L,\mathrm{NOM}}$, as shown in Fig. 4. The maximum voltage is usually dictated by the rating of the devices, connected at the dc-link side, while the minimum voltage is forced by either load unit or protection circuits of the converter (in order to prevent overcurrents). Hence, the dc link must be kept between these limits in addition of some safety bands ($V_{L,\mathrm{MIN}}$ to $V_{L,\mathrm{MAX}}$). In such a case, the maximum current drawn by the load is given by

$$I_{LC,\mathrm{MAX}} = \frac{P_{LC,\mathrm{MAX}}}{V_{L,\mathrm{MIN}}} \tag{3}$$

while the maximum current supplied by the load is as follows:

$$I_{LS,\mathrm{MAX}} = \frac{P_{LS,\mathrm{MAX}}}{V_{L,\mathrm{MIN}}}. \tag{4}$$

To conclude, voltage, power, and energy are three main vehicle load requirements, which must be instantaneously satisfied by the sources/storage units in order to ensure correct operation.

III. Battery-Powered Electric Vehicles

The battery-powered electric vehicle powertrain is shown in Fig. 5. Since the battery is the only source, it must instantaneously satisfy all the three aforementioned vehicle load requirements.

In order to fulfill the voltage requirement, the battery pack voltage must be matched to the voltage operating range of the load. A typical battery may be closely represented by its Thevenin equivalent, where the Thevenin voltage V_B is a function of the battery state of charge, state of health, temperature, humidity, etc. When the battery is fully charged, V_B is maximal; while discharging, the value of V_B is reduced. The internal resistance r_B is also a nonconstant operation-dependent value. Hence, the battery terminal voltage is dictated by the load current I_L and must satisfy

$$V_{L,\mathrm{MIN}} < V_B - r_B I_L < V_{L,\mathrm{MAX}}. \tag{5}$$

In addition, the battery management circuitry is responsible for cutting off the power when the battery terminal voltage reaches a predetermined minimum value in order to prevent any damage of the battery. Hence, when the instantaneous load current is given by (3), the battery terminal voltage is at the lowest value. If this value is lower than either $V_{L,\mathrm{MIN}}$ or the battery management circuitry predetermined minimum value, the battery is cut off despite the residual energy (typically around 25% of energy remains unused).

In order to satisfy the power and energy requirements, the energy and power rating of the battery pack must be properly selected. The main problem of the modern technology is the separation of batteries into high energy and high power types, according to the battery capacity and maximum allowed discharge rate [26], [27]. High-energy cell advantages are expressed in terms of gravimetric and volumetric energy densities, while its disadvantages appear in terms of gravimetric and volumetric power densities. Modern electric vehicles (e.g., RC aircraft and road electric vehicles) typically employ high power battery packs, since the peak power demand is several times higher than the average demand. As a result, their energy content, and hence, the driving range/mission duration is relatively low. Therefore, the need for high power–high energy hybridization is evident and will be discussed in Section IV.

IV. Energy Storage Hybridization

In order to design hybrid energy storage, Ragone plot [28] is usually employed in order to classify the available energy sources according to their power/energy density. The Ragone plot presenting the modern bidirectional energy sources and fuel cells is shown in Fig. 6 [18]. According to Fig. 6, high-energy Li-ion batteries possess the highest energy density of the modern batteries (200–250 $\mathrm{W{\cdot}h{\cdot}kg^{-1}}$) and relatively poor power density (400–500 $\mathrm{W{\cdot}kg^{-1}}$). Note the extremely high energy and lower power density of fuel cells, which cannot be used as energy storage because they support unidirectional power flow only and will be used as range extenders. At the other

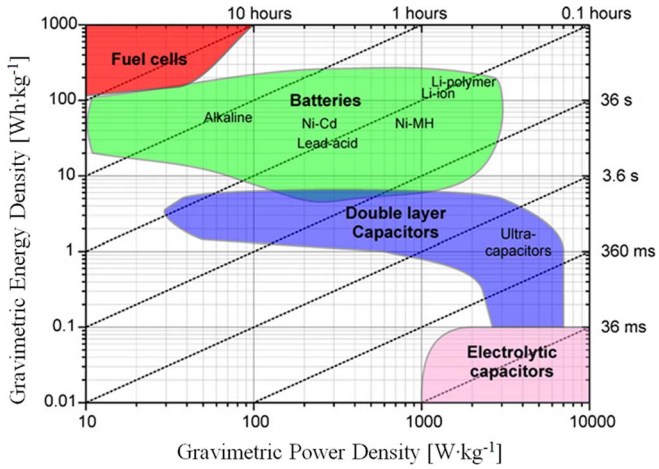

Fig. 6. Ragone plot [18].

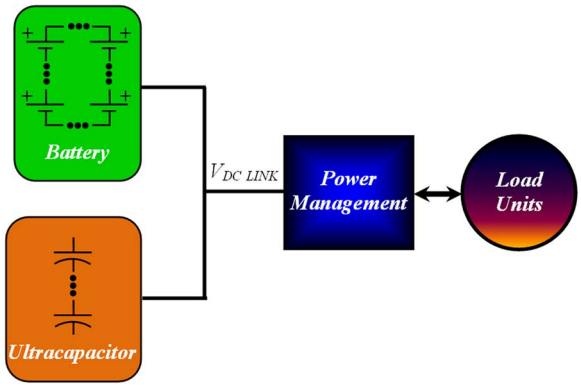

Fig. 7. Passive hybrid topology.

hand, ultracapacitors possess an extremely high power density (around 5000 W·kg^{-1}) at the expense of a very low energy density (around 5 W·h·kg^{-1}). In addition, the ultracapacitor internal resistance is much lower than the high-energy battery resistance (order of magnitude). As a result, the ultracapacitor possesses much higher charging/discharging efficiency [29]. Hence, the hybridization of high-energy Li-ion batteries and ultracapacitors seems to result in a high performance energy storage unit. The desired operation of such a hybrid is as follows: the battery should supply a nearly constant (average) load current, reducing the internal I^2R losses, and preventing battery terminal voltage dips, while the ultracapacitor should match the battery to the load by supplying the dynamic current with zero average. The rest of the section briefly describes passive, semiactive and active Li-ion–ultracapacitor hybrids. For a more comprehensive review, the reader is referred to [51].

A. Passive Hybrids

The passive hybrid is, by far, the most common battery–ultracapacitor hybrid, studied by many researchers and employed in commercial products. In the passive hybrid topology, the battery and ultracapacitor packs are connected in parallel directly to the dc link, as shown in Fig. 7. The obvious advantages of this topology are the simplicity and the lack of power

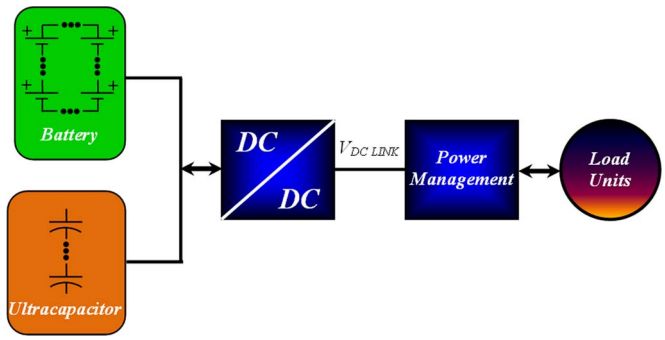

Fig. 8. Parallel semiactive hybrid energy storage powertrain.

electronics and control circuitry, reducing the overall energy, and power density. The main disadvantage is the uncontrolled current flow, determined only by the sources impedances and low utilization of the ultracapacitor. The usable energy of the ultracapacitor $E_{\rm UC}$ is limited in the passive hybrid configuration (neglecting the capacitor ESR) by the battery terminal voltage to

$$E_{\rm UC} \cong \frac{1}{2}C(V_{\rm BAT,MAX}^2 - V_{\rm BAT,MIN}^2) \tag{6}$$

where $V_{\rm BAT,MAX}$ is the maximum battery voltage (at minimum battery current) and $V_{\rm BAT,MIN}$ is the minimum battery voltage (at maximum battery current). Recall that for a correct operation, these voltage values are fairly close, and hence, the usable energy of the ultracapacitor is low. As a result, if the maximum dynamic powertrain energy $E_{\rm SDYN,MAX}$ (see Fig. 3) is higher than $E_{\rm UC}$, the ultracapacitor bank must be increased by connecting more capacitors in parallel.

B. Semiactive Hybrids

In a semiactive hybrid, a dc–dc converter is employed, in addition to the battery and ultracapacitor banks. There are three possible semiactive configurations: battery active, capacitor active, and parallel active.

1) Parallel Semiactive Hybrid: In the parallel semiactive configuration, a dc–dc converter is placed between the parallel branch of battery/ultracapacitor and the dc link, as shown in Fig. 8. This configuration improves the passive hybrid topology by satisfying the voltage requirement of the load via maintaining the dc-link voltage at its nominal value despite variations of the battery/ultracapacitor voltage. In addition, it allows a mismatch between the battery voltage (and hence, the ultracapacitor voltage rating) and the load. Nevertheless, it does not change the fact that the battery supplies part of the dynamic current and the ultracapacitor available energy is still limited. Another drawback is the need for a full rating dc–dc converter.

2) Capacitor Semiactive Hybrid: In the capacitor semiactive configuration, the dc–dc converter is placed between the capacitor and dc link, as shown in Fig. 9. Such a topology allows decoupling between the ultracapacitor and the dc-link voltages, thus improving the utilization of the ultracapacitor energy. The topology is useful in vehicles with large amount of regenerative braking energy. The typical ultracapacitor voltage operating

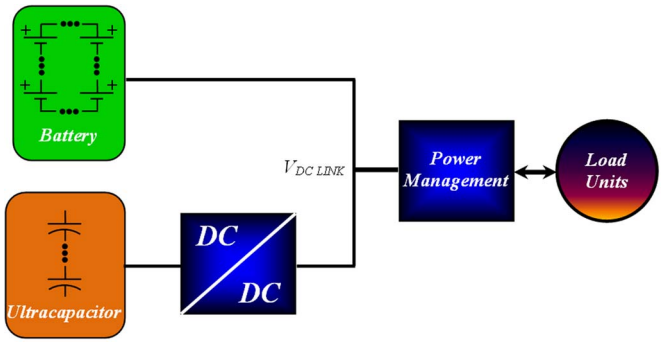

Fig. 9. Capacitor semiactive hybrid energy storage powertrain.

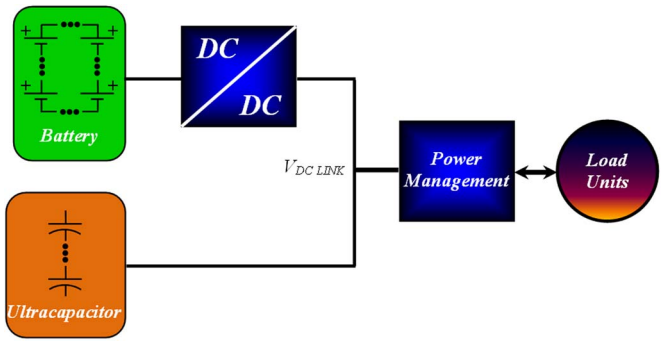

Fig. 10. Battery semiactive hybrid energy storage powertrain.

range is 50% to 100% of its rated voltage, allowing utilization of 75% of the overall available energy.

The capacitor voltage is normally controlled to a set point value, dividing the available energy into two, usually equal parts. This allows utilizing 37.5% of the overall available energy for sudden acceleration (consumed load power) or regenerative braking (supplied load power). The main disadvantages of the approach are the high rating of the dc–dc converter and the fact that the battery still supplies part of the dynamic currents in some cases.

3) Battery Semiactive Hybrid: In the battery semiactive configuration, the dc–dc converter is connected between the battery and the dc link, as shown in Fig. 10. The main advantage of such a topology is the ability to maintain the battery current at a near constant value despite the load current variations. This allows significant improving the battery performance in terms of lifetime, energy efficiency, and temperature. In addition, the voltage matching between the battery and the dc link is no longer required. The dc–dc converter rating can be chosen, according to the average load power (several times lower than the peak power, as stated earlier). The main disadvantage of the topology is the variation of the dc-link voltage during capacitor charging/discharging. The value of the capacitor must be chosen such that when the maximum charging/discharging energy is drawn from the capacitor, its voltage remains between the permissible values of the load voltage range. This can lead to a very large capacitance value. In addition, the capacitor voltage rating must be matched to the load voltage.

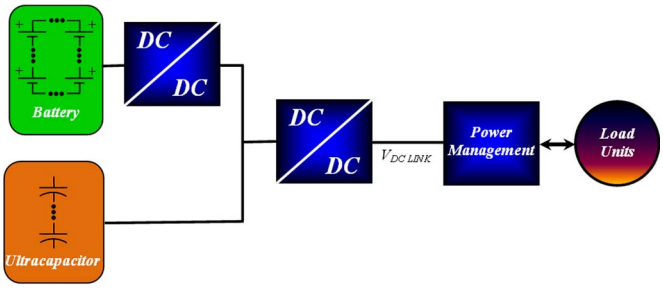

Fig. 11. Series active hybrid energy storage powertrain.

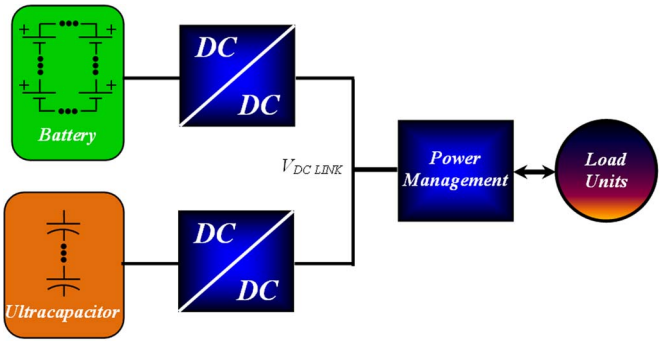

Fig. 12. Parallel active hybrid energy storage powertrain.

C. Active Hybrids

In active hybrids, two dc–dc converters are employed, in addition to the battery and ultracapacitor banks. There are two possible active configurations: series active and parallel active.

1) Series Active Hybrid: The topology is an enhancement of the battery semiactive hybrid, as shown in Fig. 11. It solves the problems of ultracapacitor voltage variation and matching by placing an additional dc–dc converter between the ultracapacitor and the dc link. The main disadvantages of the topology are the addition of a full rating dc–dc converter and reduced efficiency, since there are two conversion stages between the battery and the dc link.

2) Parallel Active Hybrid: This topology is, by far, the optimal active hybrid, reported in literature. It solves the problems of ultracapacitor voltage variations and matching by placing a dc–dc converter between the ultracapacitor and the dc link. In addition, it allows a nearly constant current flow from the battery as well as voltage mismatch between the battery and the dc link by placing a dc–dc converter between the battery and the dc link. The topology is shown in Fig. 12. The main disadvantage of the topology is the utilization of two dc–dc converters, one rated at the load average power and another rated according to the dynamic peak power, bringing complexity, control effort, and additional losses into the system.

V. Range Extension

As stated in Section I, the concept of the range extension is utilizing high-energy sources to enhance the vehicle endurance. An interesting outcome is derived from observing Fig. 3. If it is desired to increase the vehicle operating range by going over

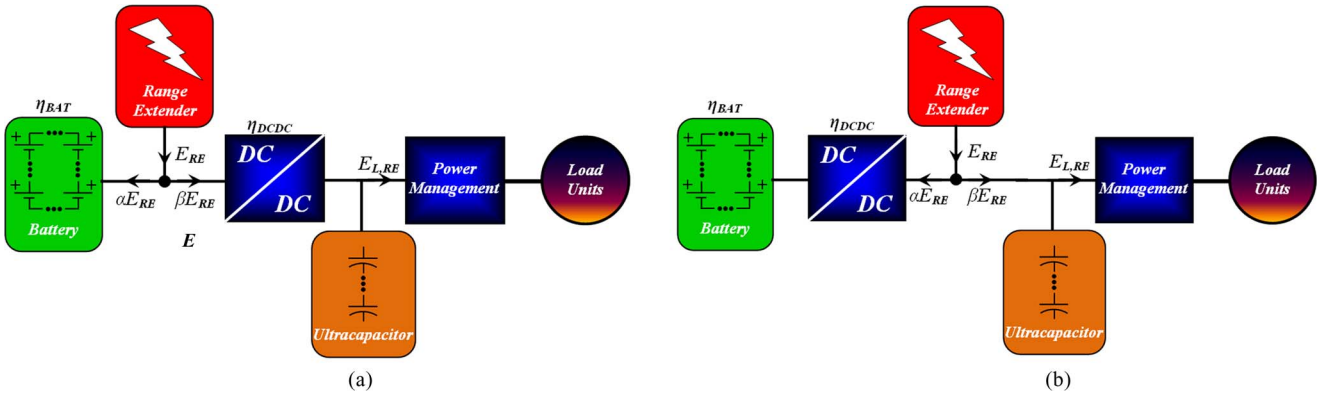

Fig. 13. Range extender connection. (a) Battery (b) DC link.

and over the presented consumption profile, only the energy requirement changes. The power and voltage requirements do not change. Hence, the range extender must be able to inject a nearly constant power to the system in order to enhance the vehicle operating range. However, this is not possible with all the range extenders, as will be explained later. Meanwhile, the first question is: what is the optimal point of connecting a range extender in case of a hybrid energy source?

Consider, for example, a battery semiactive hybrid powertrain (see Fig. 10). There are two possible points of connecting a range extender: battery and dc link, as shown in Fig. 13(a) and (b), respectively. Assume that the part of the range extender energy E_{RE} is routed to charge the battery (αE_{RE}) and the rest (βE_{RE}) goes to the load ($\alpha, \beta \leq 1$). The battery charge/discharge efficiency and the dc–dc converter efficiency are denoted as η_{BAT} and $\eta_{\mathrm{dc-dc}}$, respectively. The energy routed to the battery is eventually delivered to the load. Hence, in case of range extender connected to the battery, the range extender energy delivered to the load $E_{L,\mathrm{RE}}$ is given by

$$E_{L,\mathrm{RE}} = E_{\mathrm{RE}}(\beta + \alpha\eta_{\mathrm{BAT}})\eta_{\mathrm{dc-dc}} \tag{7}$$

while in case of range extender connected to the dc link, this energy is obtained as follows:

$$E_{L,\mathrm{RE}} = E_{\mathrm{RE}}(\beta + \alpha\eta_{\mathrm{BAT}}\eta_{\mathrm{dc-dc}}^2). \tag{8}$$

Comparing (7) and (8) reveals that the connection to the dc link is preferable if the following holds:

$$(1 - \eta_{\mathrm{dc-dc}})(\beta - \alpha\eta_{\mathrm{BAT}}\eta_{\mathrm{dc-dc}}) > 0. \tag{9}$$

Since the efficiency is always less than unity, (9) can be further simplified into

$$\beta > \alpha\eta_{\mathrm{BAT}}\eta_{\mathrm{dc-dc}}. \tag{10}$$

The meaning of (10) is as follows: if the majority of the range extender energy is routed to the load, it should be connected to the dc link. However, all the range extender energy is eventually delivered to the load. Hence, the main conclusion is: in order to increase the efficiency, the battery of the range-extender-based powertrain should not be charged during the mission/driving cycle. All the range extender energy should be routed to the load by power management circuitry.

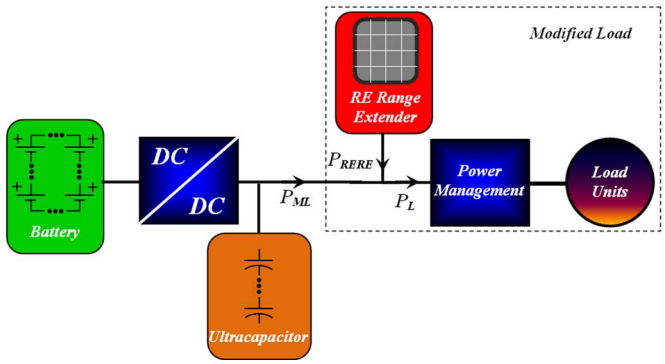

Fig. 14. RERE operational strategy.

The modern range extenders can be divided into two main groups: renewable energy range extenders (RERE) and fuel-based range extenders (FBRE). The rest of this section describes the operational strategies of the two kinds of range extenders.

A. Renewable Energy Range Extenders

The most feasible RERes are, by far, solar arrays. Solar arrays have been used in road vehicles [30], unmanned aerial vehicles [31], and rickshaws [32]. The main disadvantage of solar arrays is the strict dependence of the output power on the solar irradiance and ambient temperature. This kind of range extenders can be used during sunny days for several hours only. Even during sunny hours, the power output changes according to the weather conditions and is highly random. Hence, it cannot be operated as a constant power source and should be operated using maximum power point tracking (MPPT) strategy in order to extract the maximum available solar energy. Since the solar array power P_{RE} is uncontrolled, the rest of the system should perceive the solar array as an additional regenerative load, as shown in Fig. 14. Adopting such a strategy allows combining of the vehicle load and the range extender into a single-modified load unit, since both are random and uncontrolled. Such an operation strategy allows reducing the overall load seen by the energy storage to

$$P_{\mathrm{ML}}(t) = P_L(t) - P_{\mathrm{RE}}(t). \tag{11}$$

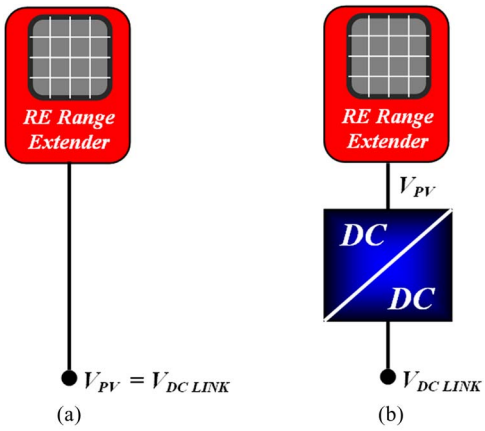

Fig. 15. RERE connection. (a) Direct. (b) Converter-based.

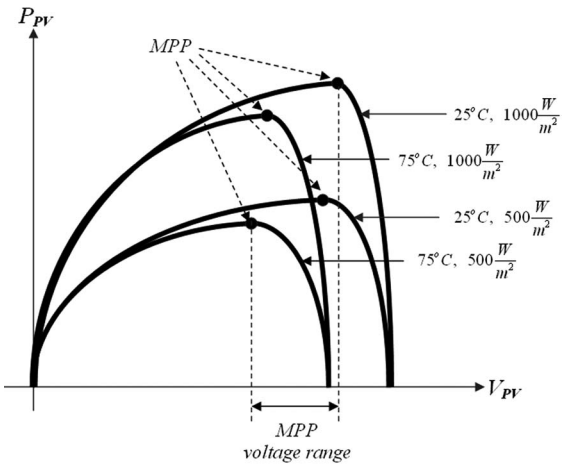

Fig. 16. Typical solar array characteristics.

Note that reduction in both average and dynamic load powers are obtained. One possible hazardous outcome occurs, when the propulsion load is regenerating and the range extender supplies large amount of energy at the same time. In such a case, the amount of energy supplied to the energy storage may be higher than rated and the range extender output should be temporarily reduced. Additional point of the discussion is the connection topology of the solar array to the dc link: direct versus converter-based (see Fig. 15). In order to understand the tradeoffs, power versus voltage characteristics of a typical solar array for different irradiation levels and temperatures are shown in Fig. 16 [33]. Obviously, the MPP corresponds to different voltages at different weather conditions. Hence, if the direct connection is chosen, the solar array should be matched to the dc link voltage such that the dc-link operating voltage resides inside the MPP voltage range.

However, since both the dc-link voltage and the ambient conditions change are uncorrelated, the operation point will always deviate from the MPP and typically around 15% of available energy is lost. The main advantage of the direct topology is the simplicity and reduced power electronics circuitry.

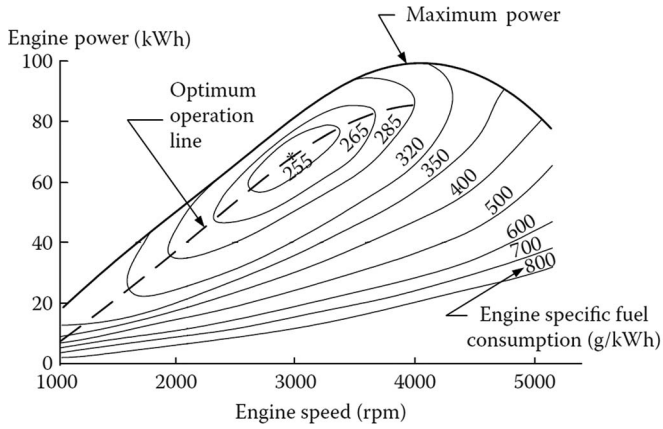

Fig. 17. Typical ICE operational characteristics [46].

In case of the converter-based connection, the array is not required to be matched to the dc-link voltage. In addition, the converter will operate using MPPT strategy, extracting the maximum power for any weather condition at the expense of power electronics, control circuitry, and converter losses.

B. Fuel-Based Range Extenders

Since the conventional fuels possess extremely high energy density, internal combustion engine (ICE)/microturbine—generators and fuel cells are perfect candidates for FBREs. ICE-based range extenders have been recently proposed in different configurations [34]–[39] and the results obtained were pretty promising. The main disadvantages of such devices are polluting emissions and noise. Fuel cells are considered as a promising alternative for combustion engines in road, naval, and aerial vehicles, as shown by several recent researches [40]–[46]. Quiet operation and near-zero emissions are the reason fuel cells are considered as an attractive energy source of the future.

The operating strategy for the FBRE is different than the REREs, since the MPP of the fuel-based devices is not the most efficient point. Fig. 17 [46] and Fig. 18 [40], respectively, present the typical operating characteristics of ICE and fuel cell. According to Figs. 17 and 18, FBRE possess an optimal operating point, called maximum efficiency point (MEP). When operating at MEP, the specific fuel consumption (amount of fuel consumed for producing 1 kW·h of electrical energy) is the lowest. Note that the power output at MEP is lower than the device rated power output. Hence, the operation strategy of the FBREs should rely on drawing a constant power from the range extender, corresponding to the minimum specific fuel consumption, despite the dc-link voltage and load variations. This is why the FBRE should be connected to the dc link via a power electronic converter, as shown in Fig. 19 [47], [48].

When operating as a system, if the FBRE supplies a constant power P_{OPT} according to the MEP (see Fig. 20), the remaining power supplied by the energy storage P_{ES} is as follows:

$$P_{\mathrm{ES}} = P_{\mathrm{ML}}(t) - P_{\mathrm{OPT}} = P_L(t) - P_{\mathrm{RE}}(t) - P_{\mathrm{OPT}}. \quad (12)$$

To conclude, the FBRE supplies controlled average power, while the RERE supplies uncontrolled average and dynamic powers.

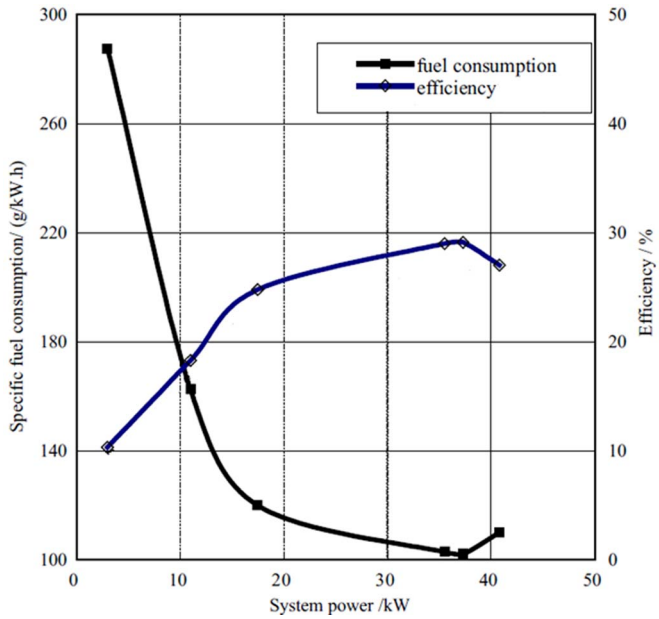

Fig. 18. Typical fuel cell operational characteristics [40].

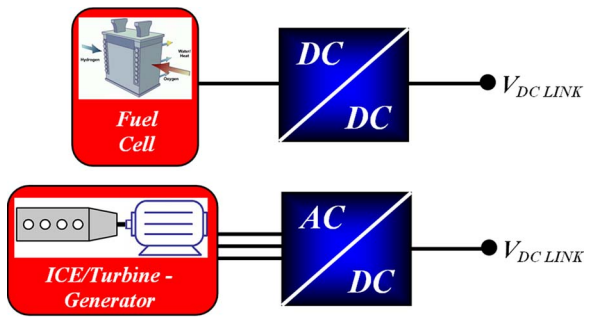

Fig. 19. FBREs connection to the dc link.

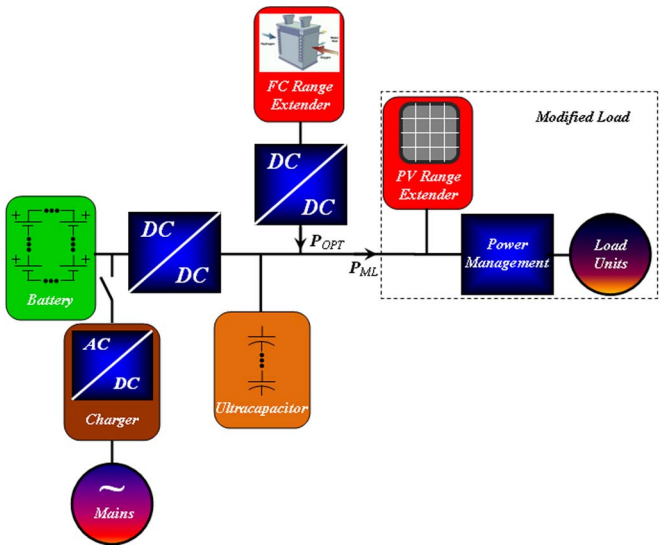

Fig. 20. Typical system structure.

The FBRE can be operated in a different point; however, this operation would not be efficient. If the FBRE power reduction is required for some reason, the ON–OFF strategy should be employed [46], where the FBRE either operates at MEP or is shut down with a duty cycle resulting in the desired average power. A typical powertrain of a battery-powered vehicle with range extenders is shown in Fig. 20. The system employs a battery semiactive hybrid, reinforced by a fuel-cell-based FBRE and a solar-array-based RERE with direct connection to the dc link. When the vehicle is resting, the battery and ultracapacitor are usually charged from ac mains via an on-board (in case of ground vehicle) and off-board (in case of aerial or underwater vehicles) charger, realized using a controlled ac/dc converter. Note that the system (see Fig. 20) perfectly resembles a dc microgrid structure [49], [50], shown in Fig. 1.

VI. Conclusion

This paper presented an overview of different topologies for hybrid powertrains for range extenders reinforced battery-powered vehicles. The disadvantages of conventional modern batteries were revealed and battery–ultracapacitor hybrids were proposed as a possible solution. Different topologies of hybrids were discussed, presenting advantages and disadvantages of each configuration. Active hybrids were shown to outperform the passive and semiactive topologies at the expense of complex circuitry and control effort.

Two types of range extenders, renewable energy and fuel-based units, were discussed. The operation strategy was shown to be different for each range extender type. For the renewable-energy-based range extender, MPPT operating strategy was shown to be preferable. Such a strategy allowed the rest of system to perceive the RERE as an additional regenerative load. Solar array was given as an example of a RERE and the possible connection topologies were discussed. For the FBRE, MEP tracking strategy was chosen in order to achieve the lowest specific fuel consumption. Fuel cells and ICEs were presented as possible candidates of FBREs. The complete powertrain was shown to resemble a dc microgrid with source, storage, and load units connected through power management circuitry to a common dc link.

References

[1] D. Lee, G. Pitari, V. Grewe, K. Gierens, J. Penner, A. Petzold, M. Prather, U. Schumann, A. Bais, T. Berntsen, D. Iachetti, and R. Sausen, "Transport impacts on atmosphere and climate," *Atmos. Environ.*, vol. 44, no. 37, pp. 4735–4771, 2010.

[2] A. Emadi, K. Rajashekara, S. Williamson, and S. Lukic, "Topological overview of hybrid electric and fuel cell vehicular power system architectures and configurations," *IEEE Trans. Veh. Technol.*, vol. 54, no. 3, pp. 763–770, May 2005.

[3] S. Williamson and A. Emadi, "Comparative assessment of hybrid electric and fuel cell vehicles based on comprehensive well-to-wheels efficiency analysis," *IEEE Trans. Veh. Technol.*, vol. 54, no. 3, pp. 856–863, May 2005.

[4] A. Emadi, S. Williamson, and A. Khaligh, "Power electronics intensive solutions for advanced electric, hybrid electric, and fuel cell vehicular power systems," *IEEE Trans. Power Electron.*, vol. 21, no. 3, pp. 567–577, May 2006.

[5] S. Williamson, M. Lukic, and A. Emadi, "Comprehensive drive train efficiency analysis of hybrid electric and fuel cell vehicles based on

motor-controller efficiency modeling," *IEEE Trans. Power Electron.*, vol. 21, no. 3, pp. 730–740, May 2006.
[6] S. Williamson, A. Emadi, and K. Rajashekara, "Comprehensive efficiency modeling of electric traction motor drives for hybrid electric vehicle propulsion applications," *IEEE Trans. Veh. Technol.*, vol. 56, no. 4, pp. 1561–1572, Jul. 2007.
[7] D. Gao and A. Emadi, "Modeling and simulation of electric and hybrid vehicles," in *Proc. IEEE*, Apr. 2007, vol. 95, no. 4, pp. 729–745.
[8] A. Emadi, Y. Lee, and K. Rajashekara, "Power electronics and motor drives in electric, hybrid electric, and plug in electric vehicles," *IEEE Trans. Ind. Electron.*, vol. 55, no. 6, pp. 2237–2245, Jun. 2008.
[9] F. Mapelli, D. Tarsitano, and M. Mauri, "Plug in hybrid electric vehicle: Modeling, prototype realization and inverter losses reduction analysis," *IEEE Trans. Ind. Electron.*, vol. 57, no. 2, pp. 598–607, Feb. 2010.
[10] Y. Gao and M. Ehsani, "Design and control methodology of plug in hybrid electric vehicles," *IEEE Trans. Ind. Electron.*, vol. 57, no. 2, pp. 633–640, Feb. 2010.
[11] C. Chan, A. Bouscayrol, and K. Chen, "Electric, hybrid and fuel cell vehicles: Architectures and modeling," *IEEE Trans. Veh. Technol.*, vol. 59, no. 2, pp. 589–598, Feb. 2010.
[12] A. Emadi and M. Ehsani, "Aircraft power systems: technology, state of the art, and future trends," *IEEE Aerosp. Electron. Syst. Mag.*, vol. 15, no. 1, pp. 28–32, Jan. 2000.
[13] A. Sehra and W. Whitlow, "Propulsion and power for 21st century aviation," *Prog. Aerosp. Sci.*, vol. 40, no. 4, pp. 199–235, 2004.
[14] N. Lapena-Rey, J. Mosquera, E. Bataller, F. Orti, C. Dudfield, and A. Orsillo, "Environmental friendly power sources for aerospace applications," *J. Power Sources*, vol. 181, pp. 353–362, 2008.
[15] E. Bataller-Planes, N. Lapena-Rey, J. Mosquera, F. Orti, J. Oliver, O. Garcia, F. Moreno, J. Portilla, Y. Torroja, M. Vasic, S. Huerta, M. Trocki, P. Zumel, and J. Cobos, "Power balance of a hybrid power source in a power plant for a small propulsion aircraft," *IEEE Trans. Power Electron.*, vol. 24, no. 12, pp. 2856–2866, Dec. 2009.
[16] B. Skinner, G. Parks, and P. Palmer, "Comparison of submarine drive topologies using multiobjective genetic algorithms," *IEEE Trans. Veh. Technol.*, vol. 58, no. 1, pp. 57–68, Jan. 2009.
[17] J. Apsley, A. Gonzalez-Villasenor, M. Barnes, A. Smith, S. Williamson, J. Schuddebeurs, P. Norman, C. Booth, G. Burt, and J. McDonald, "Propulsion drive models for full electric marine propulsion systems," *IEEE Trans. Ind. Appl.*, vol. 45, no. 2, pp. 676–684, Mar./Apr. 2009.
[18] Q. Cai, D. Brett, D. Browning, and N. Brandon, "A sizing design methodology for hybrid fuel cell power systems and its application to an unmanned underwater vehicle," *J. Power Sources*, vol. 195, pp. 6559–6569, 2010.
[19] M. Kepros and W. van Schalkwijk, "Back to the future? Return of the hybrid," *Electrochem. Soc. Interf.*, vol. 11, pp. 34–37, 2002.
[20] A. Ferreira, J. Pomilio, G. Spiazzi, and L. Silva, "Energy management fuzzy logic supervisory for electric vehicle power supplies system," *IEEE Trans. Power Electron.*, vol. 23, no. 1, pp. 107–115, Jan. 2008.
[21] P. Biczel, "Power electronic converters for DC microgrids," in *Proc. IEEE Compat. Power Electron. Conf.*, 2007, pp. 1–6.
[22] F. Katiraei, R. Iravani, N. Hatziagyriou, and A. Dimeas, "Microgrids management," *IEEE Power Energy Mag.*, vol. 6, no. 3, pp. 54–65, May/Jun. 2008.
[23] C. Sao and P. Lehn, "Control and power management of converter fed microgrids," *IEEE Trans. Power Syst.*, vol. 23, no. 3, pp. 1088–1098, Aug. 2008.
[24] J. Wang and D. Howe, "A power shaping stabilizing control strategy for DC power systems with constant power systems," *IEEE Trans. Power Electron.*, vol. 23, no. 6, pp. 2982–2989, Nov. 2008.
[25] M. Ehsani, Y. Gao, and J. Miller, "Hybrid electric vehicles: Architecture and motor drives," in *Proc. IEEE*, Apr. 2007, vol. 95, no. 4, pp. 719–728.
[26] D. Corson, "High power battery systems for hybrid vehicles," *J. Power Sources*, vol. 105, pp. 110–113, 2002.
[27] S. Lukic, J. Cao, R. Bansal, F. Rodrigues, and A. Emadi, "Energy storage systems for automotive applications," *IEEE Trans. Ind. Electron.*, vol. 55, no. 6, pp. 2258–2267, Jun. 2008.
[28] T. Christen and M. Carlen, "Theory of ragone plots," *J. Power Sources*, vol. 91, no. 2, pp. 210–216, 2000.
[29] A. Burke, "Batteries and ultracapacitors for electric, hybrid, and fuel cell vehicles," in *Proc. IEEE*, Apr. 2007, vol. 95, no. 4, pp. 806–820.
[30] J. Kimball, B. Kuhn, and R. Balog, "A system design approach for unattended solar energy harvesting supply," *IEEE Trans. Power Electron.*, vol. 24, no. 4, pp. 952–962, Apr. 2009.
[31] J. Shiau, D. Ma, P. Yang, G. Wang, and J. Gong, "Design of a solar power management system for an experimental UAV," *IEEE Trans. Aerosp. Electron. Syst.*, vol. 45, no. 4, pp. 1350–1360, Oct. 2009.
[32] P. Mulhall, S. Lukic, S. Wirasingha, Y. Lee, and A. Emadi, "Solar-assisted electric auto rickshaw three wheeler," *IEEE Trans. Veh. Technol.*, vol. 59, no. 5, pp. 2298–2307, Jun. 2010.
[33] M. Villalva, J. Gazoli, and E. Filho, "Comprehensive approach to modeling and simulation of photovoltaic arrays," *IEEE Trans. Power Electron.*, vol. 24, no. 5, pp. 1198–1208, May 2009.
[34] B. Powell and T. Pilutti, "A range extender hybrid vehicle dynamic model," in *Proc. IEEE Conf. Decis. Control*, 1994, vol. 3, pp. 2736–2741.
[35] A. Schmidhofer, G. Zhang, and H. Weiss, "Range extender optimization for electrical vehicles," in *Proc. IEEE Int. Conf. Ind. Technol.*, 2003, vol. 1, pp. 570–574.
[36] B. He and M. Yang, "Robust LPV control of diesel auxiliary power unit for series hybrid electric vehicle," *IEEE Trans. Power Electron.*, vol. 21, no. 3, pp. 791–798, May 2006.
[37] K. Imai, T. Ashida, Y. Zhang, and S. Minami, "EV range extender: Better mileage than plug-in hybrid?," in *Proc. IEEE Veh. Power Propulsion Conf.*, 2008, pp. 1–3.
[38] M. van Wieringen, M. Bernacki, and R. Pop-Iliev, "Design and development of a plug in by wire(less) hydrogen internal combustion engine extended range electric vehicle," in *Proc. IEEE Veh. Power Propulsion Conf.*, 2008, pp. 1–8.
[39] F. Yunzhou, Z. Han, P. Qingfeng, and L. Shijiang, "Research on generator set control of range extender pure electric vehicles," in *Proc. Asia-Pacific Power Energy Eng. Conf.*, 2010, pp. 1–4.
[40] P. Pei, M. Ouyang, Q. Lu, H. Huang, and X. Li, "Testing of an automotive fuel cell system," *Int. J. Hydrogen Energy*, vol. 29, pp. 1001–1007, 2004.
[41] K. Rajashekara, J. MacBain, and M. Grieve, "Evaluation of SOFC hybrid systems for automotive propulsion applications," in *Proc. IEEE Ind. Appl. Conf.*, 2006, vol. 3, pp. 1593–1597.
[42] P. Aguiar, D. Brett, and N. Brandon, "Solid oxide fuel cell/gas turbine hybrid system analysis for high altitude long endurance unmanned aerial vehicles," *Int. J. Hydrogen Energy*, vol. 33, pp. 7214–7223, 2008.
[43] C. Ramos-Paja, C. Bordons, A. Romero, R. Giral, and L. Martinez-Salamero, "Minimum fuel consumption strategy for PEM fuel cells," *IEEE Trans. Ind. Electron.*, vol. 56, no. 3, pp. 685–696, Mar. 2009.
[44] G. Offer, D. Howey, M. Contestabile, R. Clague, and N. P. Brandon, "Comparative analysis of battery electric, hydrogen fuel cell and hybrid vehicles in a future sustainable road transport system," *Energy Policy*, vol. 38, pp. 24–29, 2010.
[45] M. Cordner, M. Matian, G. Offer, T. Hanten, E. Spofforth-Jones, S. Tippets, A. Agrawal, L. Bannar-Martin, L. Harito, A. Johnson, R. Clague, F. Marquis, A. Heyes, Y Hardalupas, and N. Brandon, "Designing, building, testing and racing a low cost fuel cell range extender for a motorsport application," *J. Power Sources*, vol. 195, no. 23, pp. 7838–7848, 2010.
[46] M. Ehsani, Y. Gao, and A. Emadi, *Modern Electric, Hybrid Electric and Fuel Cell Vehicles: Fundamentals, Theory and Design*, 2nd ed. Boca Raton, FL: CRC Press, 2010.
[47] L. Palma and P. Enjeti, "A modular fuel cell, modular DC-DC converter concept for high performance and enhanced reliability," *IEEE Trans. Power Electron.*, vol. 24, no. 6, pp. 1437–1443, Jun. 2009.
[48] S.-Y. Park, C.-L. Chen, and J.-S. Lai, "A wide range active and reactive power flow controller for a SOFC power condition system," *IEEE Trans. Power Electron.*, vol. 23, no. 6, pp. 2703–2709, Nov. 2008.
[49] E. Barklund, N. Pogaku, M. Prodanovic, C. Hernandez-Aramburo, and T. Green, "Energy management in autonomous microgrids using stability constrained droop control of inverters," *IEEE Trans. Power Electron.*, vol. 23, no. 5, pp. 2346–2352, Sep. 2008.
[50] A. Payman, S. Pierfederici, and F. Meibody-Tabar, "Energy management in a fuel cell/supercapacitor multisource/multiload electrical hybrid system," *IEEE Trans. Power Electron.*, vol. 24, no. 12, pp. 2681–2691, Dec. 2009.
[51] A. Kuperman and I. Aharon, "Battery–ultracapacitor hybrids for pulsed current loads: A review," *Renew. Sustain. Energy Rev.*, vol. 15, pp. 981–992, 2011.

Author's photographs and biographies not available at the time of publication.